

Growth Inhibition of Ovarian Tumor-Initiating Cells by Niclosamide

Yi-Te Yo^{1,2}, Ya-Wen Lin^{2,3}, Yu-Chi Wang^{1,2}, Curt Balch^{5,6}, Rui-Lan Huang¹, Michael W.Y. Chan⁸, Huey-Kang Sytwu³, Chi-Kuan Chen⁴, Cheng-Chang Chang¹, Kenneth P. Nephew^{5,6,7}, Tim Huang⁹, Mu-Hsien Yu¹, and Hung-Cheng Lai^{1,2}

Abstract

A recent hypothesis for cancer chemoresistance posits that cytotoxic survival of a subpopulation of tumor progenitors drives the propagation of recurrent disease, underscoring the need for new therapeutics that target such primitive cells. To discover such novel compounds active against drug-resistant ovarian cancer, we identified a subset of chemoresistant ovarian tumor cells fulfilling current definitions of cancer-initiating cells from cell lines and patient tumors using multiple stemness phenotypes, including the expression of stem cell markers, membrane dye efflux, sphere formation, potent tumorigenicity, and serial tumor propagation. We then subjected such stem-like ovarian tumor-initiating cells (OTIC) to high-throughput drug screening using more than 1,200 clinically approved drugs. Of 61 potential compounds preliminarily identified, more stringent assessments showed that the antihelminthic niclosamide selectively targets OTICs *in vitro* and *in vivo*. Gene expression arrays following OTIC treatment revealed niclosamide to disrupt multiple metabolic pathways affecting biogenetics, biogenesis, and redox regulation. These studies support niclosamide as a promising therapy for ovarian cancer and warrant further preclinical and clinical evaluation of this safe, clinically proven drug for the management of this devastating gynecologic malignancy. *Mol Cancer Ther*; 11(8); 1703–12. ©2012 AACR.

Introduction

Ovarian cancer is the most lethal gynecologic malignancy and the fifth-most cause of overall cancer death of women in developed countries (1). The majority of women diagnosed with advanced-stage epithelial ovarian cancer experience associated with the development of chemoresistance and platinum-resistant tumor recurrence, a pathology that is uniformly fatal (2). An increasingly accepted cancer stem cell hypothesis regards tumors as caricatures of normal organs, possessing a hierarchy of

cell types, at various stages of aberrant differentiation, descended from precursor tumor-initiating cells (TIC) cells that are highly resistant to conventional cytotoxics (3, 4).

Several TICs have now been isolated, in ovarian and other solid tumor malignancies, and our group also successfully isolated ovarian TICs (OTIC) from human tumors that specifically express the surface markers CD44 (a hyaluronate receptor) and CD117 (c-Kit or stem cell factor receptor; ref. 5). Other reported OTIC surface markers include CD133, CD24, CD44, and Myd88 (6–8). Although this approach has proved successful for characterizing a number of solid tumor progenitor cells, shortcomings include uncertainty of the precise roles of the specific surface markers (with regard to tumor potency) and insufficient isolation of cells for use in drug screening assessments (9).

In addition to cell-surface markers, some marker-free methods have also been applied to enrich TICs. Similar to hematopoietic and other somatic tissue stem cells, TICs express various ATP-binding cassette (ABC) transporters, including MDR1, ABCB1, and ABCG2, which confer chemoresistance via active transmembrane drug export (10). To exploit this stem cell attribute, fluorescence-activated cell sorting (FACS) of a side population of fluorescent dye-excluding cells has been used to enrich numerous normal tissue stem cells and TICs (4, 11). The side population-to-stemness link is now well substantiated by its coexistence with numerous other commonly

Authors' Affiliations: ¹Department of Obstetrics and Gynecology, Tri-Service General Hospital, ²Laboratory of Epigenetics and Cancer Stem Cells, ³Department of Microbiology and Immunology, and ⁴Graduate Institute of Life Sciences, National Defense Medical Center, Taipei, Taiwan, Republic of China; ⁵Medical Sciences Program, ⁶Indiana University Simon Cancer Center, and ⁷Department of Obstetrics and Gynecology, Indiana University School of Medicine, Indianapolis, Indiana; ⁸Department of Life Science, National Chung Cheng University, Min-Hsiung, Chia-Yi, Taiwan, Republic of China; and ⁹Department of Molecular Medicine and Institute of Biotechnology, Cancer Therapy and Research Center, University of Texas Health Science Center, San Antonio, Texas

Note: Supplementary data for this article are available at Molecular Cancer Therapeutics Online (<http://mct.aacrjournals.org>).

Corresponding Author: Hung-Cheng Lai, Department of Obstetrics and Gynecology, Tri-Service General Hospital, National Defense Medical Center, 5F, 325, Sec 2, Cheng-Gong Rd., Neihu district, Taipei city 114, Taiwan, ROC. Phone: 886-2-87923311 (ext. 10083); Fax: 886-2-87927199; E-mail: hclai@ndmctsgh.edu.tw

doi: 10.1158/1535-7163.MCT-12-0002

©2012 American Association for Cancer Research.

exploited stem cell attributes. Those progenitor phenotypes include expression of self-renewal and pluripotency-conferring transcription factors, differentiation into multiple, diverse progeny cells, activation of embryonic signaling pathways, and potent *in vivo* tumor initiation, methods that our group and others have used in the assessment of ovarian tumor progenitors (5, 12, 13). Another feature of stem/progenitor cells is their ability to self-aggregate into substrate-independent spheres, architectural structures originally discovered to be highly enriched in multipotent neural stem cells (14). Subsequently, anchorage-independent sphere formation has now been used for enrichment of stem cells from normal breast (15) and skin (16) tissues, in addition to TICs of brain (17), pancreatic (18), colon (19), and ovarian (5, 13) cancers.

Traditionally, anticancer drug development has been based on the targeting of rapidly proliferating cells, rather than cells having a capacity for self-renewal and/or differentiation, which might be more effective against malignancies possessing a tumor cell hierarchy (4, 10). It is likely that ovarian cancer is one such malignancy, based on its frequent progression to chemoresistance (20). For drug discovery targeting TICs, cell-surface marker-independent isolation offers distinct advantages in allowing relatively straightforward procedures and less biased selection of cells with specific markers. In this study, for greater stringency, we used 2 stemness selection methods, dye exclusion, and subpopulation of sphere-forming ability, while still obtaining sufficient numbers of ovarian TICs for high-throughput identification of their antagonists.

Materials and Methods

Cells and experimental animals

Human ovarian cancer cell lines OVCAR-3 and SKOV-3 were purchased from American Type Culture Collection (ATCC). The human ovarian cancer cell line A2780 and its cognate cisplatin-resistant CP70 were obtained in 2007 from Dr. Tim Huang's lab (University of Texas Health Science Center, San Antonio, TX). Earlier passages of all cell lines were maintained in several cryovials, respectively, in liquid nitrogen in our laboratory. The cell lines used were tested by Bioresource Collection and Research Center (Hsinchu, Taiwan) for identity verification by DNA profiling of short tandem repeat (STR) sequences. Briefly, 15 STR loci were tested by using the Applied Biosystems AmpFLSTR Identifier Kit (Applied Biosystems Catalog # 4322288). DNA profiles were compared manually to the ATCC and European Collection of Cell Cultures database. Cells were stored and used within 3 months after resuscitation of frozen aliquots. All cell lines were cultured in RPMI-1640 (Invitrogen) supplemented with nonessential amino acid (Invitrogen), sodium pyruvate (Invitrogen), 10% FBS (Biological Industries), and different growth factors, respectively, and plated in standard cell culture dishes (Corning). For *in vivo* tumor xenograft studies of CP70sps cells, female nonobese dia-

betic severe-combined immunodeficient (NOD/SCID) mice were obtained from the Laboratory Animal Center of the National Taiwan University (Taipei City, Taiwan). Six-week-old mice were used for experiments unless indicated otherwise. The rules of the Animal Protection Act of Taiwan were strictly followed and all animal procedures approved by the Laboratory Animal Care and Use Committee of National Defense Medical Center.

Side population spheroid cells

For side population analysis, 10^8 cells were harvested and stained with 50 $\mu\text{g}/\text{mL}$ Hoechst 33342 (Sigma). The dye exclusion phenotype (21), via membrane efflux, was confirmed by an ABCG2-specific inhibitor, GF120918. Hoechst-stained cells were subjected to FACS using a FACSAria (BD Biosciences) for collection of dye-excluding (side population) cells, which were then cultured in Ultra Low attachment plates (Corning) with serum-free Dulbecco's Modified Eagle's Medium/F12 medium containing 5 μg insulin (Sigma), 0.4% bovine serum albumin (Sigma), 10 ng/mL basic fibroblast growth factor (Invitrogen), and 20 ng/mL human recombinant EGF (Invitrogen). Side population cells were then observed for the stem cell phenotype of tumor sphere formation (22) under suspension-cultured conditions, and those spheroid-forming cells were then referred to as side population spheroid (SPS) cells. For differentiation studies, CP70sps cells were cultured in standard coated dishes (Corning) with normal media and 10% FBS.

Characterization of stem cell properties of CP70sps cells

Stem cell phenotypes of the parental CP70 and side population CP70sps cells were assessed by the expression of specific stem cell gene markers (Supplementary Table S1). SPS cells also subjected to intracytoplasmic proteins staining, following fixation by paraformaldehyde and permeation by Triton X-100. Cells were stained with antibodies against human OCT4 (Abcam), NANOG (Abcam), NESTIN (Abcam), ABCG2 (Santa Cruz Biotechnology) and then stained with fluorescence-conjugated secondary antibodies (The Jackson Laboratory) or assess the ALDH activity using ALDEFLUOR Kit (StemCell Technologies) according to the manufacturer's instructions as described previously (23) and analyzed by flow cytometry (BD Biosciences). Cells subjected to surface marker staining were incubated with CD34, CD44, or CD133 fluorescence-conjugated monoclonal antibodies (Abcam), followed by flow cytometry analysis.

Xenograft transplantation of CP70sps cells

CP70sps (P0) cells were injected intraperitoneally into NOD/SCID mice. After tumor formation, tumor nodules were harvested, mechanically dissected, enzymatically digested, and cultured in serum-free suspension to form spheroids (P1) as previously described (5). NOD/SCID mice were inoculated intraperitoneally with various numbers of CP70, CP70sps passage 0 (P0), and CP70sps

passage-1 (P1) cells. Recipients were monitored every week. Mice were euthanized when the abdomen showed swelling to observe ascites and tumor formations.

Large-scale screening of bioactive compounds

For primary screening, 1×10^3 CP70sps cells were seeded per well in a 96-well culture dish (Corning). Twenty-four hours later, cells were treated with 30 $\mu\text{mol/L}$ of more than 1,200 compound from a LOPAC library (Sigma). Three days later after treatment, the viability of treated cells was measured by CellTiter-Glo Luminescent Cell Viability Assay Kit (Promega), according to the manufacturer's instructions. Candidate compounds were then subjected to a secondary screen using a 10-fold lower dose (3 $\mu\text{mol/L}$), using 5,000 CP70sps cells seeded per well in 96-well culture dish for 24 hours.

In vitro chemosensitivity and apoptosis analysis

Ovarian cancer cells treated with various doses of cisplatin for 24 hours were used to define the chemoresistance capacity. The IC_{50} value was calculated by the cell growth using MTS-based CellTiter 96 Cell Proliferation Assay Kit (Promega). For investigation of cytochrome c release and detection of short functional apoptosis-inducing factor (AIF) fragment, niclosamide-treated CP70sps cells were harvested 48 hours later and subjected to detection using FlowCollect Cytochrome C Kit (Millipore) according to the manufacturer's instructions or to immunoblot using AIF antibody (Millipore) staining. CP70sps cells were treated with niclosamide for 72 hours and then total cells were harvested and stained with propidium iodide (PI). Samples were then analyzed for DNA content using a FACSCalibur (BD Biosciences), and relative cell-cycle distribution was analyzed using the CellQuest software (Verity Software House).

Preclinical therapeutic effects of niclosamide

NOD/SCID mice, 5 or 4 per group, were injected intraperitoneally with 1×10^4 CP70sps or 1×10^6 CP70 cells at day 0 and the experimental group then treated with niclosamide intraperitoneally (5 or 10 mg/kg/daily) for 3 weeks, followed by biweekly treatments for another 4 weeks. Mouse bodyweights were monitored every 3 days, and mice were euthanized to observe tumor nodule formation 7 weeks later, upon the development of ascites. Stem-like OTICs from patients were then peritoneally derived, as described previously (5). Five thousand peritoneally derived OTICs were then seeded in 96-well dish and treated with 3 $\mu\text{mol/L}$ of niclosamide and viability detected 3 days later by an MTS-based assay, according to the manufacturer's instructions. To test the therapeutic effects *in vivo*, NOD/SCID mice were injected intraperitoneally with 1×10^4 of CP70sps and then treated with niclosamide intraperitoneally (10 mg/kg/daily) for 3 weeks and then biweekly for another 12 weeks. Mice were euthanized upon development of measurable ascitic fluid, and tumor formation was assessed. All studies were approved by the Institutional Review Board of the Tri-

Service General Hospital, National Defense Medical Center.

Quantitative RT-PCR array, global gene expression array, and bioinformatics

CP70 and CP70sps RNA was isolated by RNeasy Mini Kits (Qiagen), suspended in the RNase-free water, and following reverse transcription to cDNA, subjected to RT² Profiler PCR Array Systems (SABioScience) for detection of stem cell gene expression using an ABI 7500 Real-Time PCR System (Applied Biosystems). For global gene expression analysis, total RNA (2 μg) from niclosamide-treated CP70 and CP70sps were isolated after various periods (2, 4, and 6 hours) and then qualified and sent to a core service unit (Genetech Biotech Co.) for whole genome expression analysis. We detected gene expression profiles on Illumina HumanWG-6 v3.0 Expression Beadchip (Illumina). The gene expression data were deposited in Gene Expression Omnibus (GEO) DataSets (accession number GSE36259). After quintile normalization, the significance of analysis microarray (SAM) algorithm was used to statistically differentiate expression patterns using a MeV 4.6.2 tool (24). PathVisio 2.0.11 (25) was then used to determine functional pathways impacted by changes in gene expression patterns, using the WikiPathways and KEGG pathways database.

Statistical analyses

Data were expressed as mean \pm SD. Differential chemoresistance in various cell lines was analyzed using the nonparametric Mann-Whitney test. *P* values less than 0.05 were considered to be statistically significant. All analyses were carried out using the statistical package in R (R version 2.13.0).

Results

Isolation and characterization of stem-like ovarian cancer cells

We first determined the side population fractions of a panel of OC cell lines by staining with Hoechst 33342 dye, followed by the isolation of Hoechst-negative cells (Fig. 1A). An ABC transport-specific inhibitor, GF120918, confirmed Hoechst dye efflux via active membrane transport (Supplementary Fig. S1A). Sphere-forming ability of the side population cells was then evaluated. CP70SP cells were screened for spheroid formation (Supplementary Fig. S1B), and those cells were thus designated CP70sps.

We next compared CP70sps and bulk culture CP70 cells for expression of various embryonic and previously reported cancer stemness markers. As shown in Fig. 1B, CP70sps cells upregulated numerous stem cell marker genes, including NANOG (5.9-fold), ALDH1 (2.2-fold), NESTIN (2.3-fold), and CD44 (1.3-fold). However, we did not observe CP70sps upregulation of CD133, a previously reported marker of ovarian cancer and/or tumor-associated endothelial, stem cells (6, 26–28). To more broadly assess gene expression in CP70sps cells, reverse

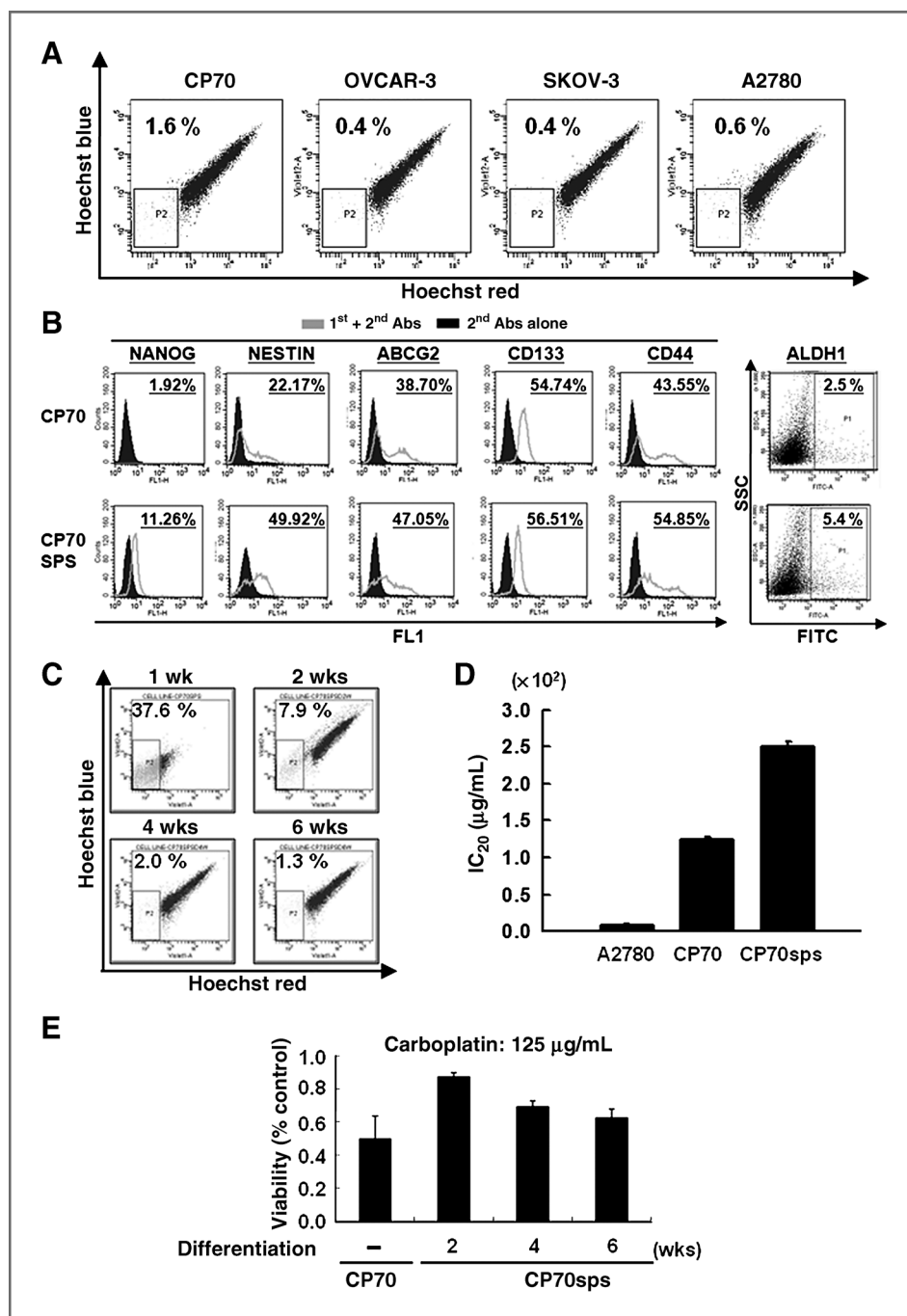


Figure 1. CP70sps cells possess tumor spheroid formation capability, express stem cell markers, repopulate, and lose chemoresistance under differentiating conditions. **A**, side population Hoechst 33342–excluding cells were quantified for 4 ovarian cancer cell lines. The dot plot shows the gated region P2 as the dye–excluding side population cells. **B**, the expression levels of stem cell markers were analyzed in both CP70 and CP70sps cells by flow cytometry. The number indicates the percentages of positively stained cells from the entire cell population. **C**, CP70sps cells cultured under standard conditions underwent proliferation and differentiation, with a progressive decrease in the side population cell fraction over time, returning to a level comparable with its parent CP70 cells in 6 weeks, indicating a repopulation property *in vitro*. Top left, most numbers indicate side population cells as a percentage of all the stained cells that were analyzed. **D**, differential platinum chemoresistance in A2780, CP70, and CP70sps. IC₅₀ dosages were determined by serial dilution dosing of carboplatin. CP70 is a selected subclone resistant to cisplatin from A2780, whereas CP70sps is further enriched from CP70. Each value represents the mean \pm SD in triplicates. **E**, loss of CP70sps cell chemoresistance under differentiating conditions, as determined by percent survival following treatment with 125 μ g/mL carboplatin (bar #1, the normal IC₅₀ of CP70 cells). All values represent means \pm SDs, in triplicate.

transcriptase PCR (RT-PCR) target arrays were used, and enrichment of several stem cell gene signatures, including the *Wnt* signal cascade (Supplementary Table S1), was observed.

As high capacity for aberrant differentiation is a foundation for the cancer stem cell hypothesis (3, 4), we next assessed whether CP70sps cells lose their stemness phenotype when exposed to differentiation-associated conditions. As shown in Fig. 1C, those culture conditions resulted in a time-dependent decrease of side population

cells, from 37.6%, after one week, to 1.3%, after 6 weeks, thus showing asymmetric cell division and differentiation potency in CP70sps cells. Platinum chemoresistance was shown in CP70sps cell, with IC₅₀ dose sensitivities being 2.0- and 20.6-fold higher than the IC₅₀ values for unselected bulk CP70 cells and their A2780 cells chemoresistant parent cell line (Fig. 1D). Analogously, after 4 to 6 weeks under differentiating culture conditions, CP70sps cells lost their chemoresistance phenotype, with an approximately 40% loss of viability (Fig. 1E).

Table 1. Tumorigenicity of CP70 OVCA cells and CP70sps OTICs

Cell type	Cell numbers					
	10 ⁷	10 ⁶	10 ⁵	10 ⁴	10 ³	10 ²
CP70	3/3 (28 d)	3/3 (40 d)	1/3 (60 d)	1/3 (60 d)	0/3	–
CP70sps P0	–	–	–	3/3 (66 d)	3/3 (70 d)	–
CP70sps P1	–	–	3/3 (21 d)	3/3 (33 d)	3/3 (41 d)	3/3 (65 d)

As the gold standard for the definitive identification of cancer stem-like cells is exponentially increased tumorigenic potential (3, 4), we directly assessed the tumorigenic capacity of CP70sps cells *in vivo*. Currently, tumorigenicity of 100 to 5,000 cells is considered sufficient to define tumor-initiating ability, with prior studies showing 100 CD117⁺ (5), 100 to 500 CD133⁺ (6), 5,000 PKH^{high/low} (29), 5,000 CD24⁺ (8), and 1,000 ALDH1^{br/low} cells (23) to sufficiently indicate ovarian cancer stemness. In this study, 1,000 CP70sps and 100 CP70sps P1 cells grew tumors, fulfilling the current definition of TICs. We did not test the tumorigenicity of one single cell in this study. Indeed, the tumorigenicity also depends on the immune background of mice (30). To more precisely recapitulate the physiologic niche of ovarian cancer (5, 20), we injected serially diluted CP70sps cells intraperitoneally into recipient NOD/SCID mice. Although only one of 3 mice grew intraperitoneal cavity tumors when injected with 10⁴ and 10⁵ CP70 cells, 3 of 3 injections of only 10³ CP70sps stem-like cells were tumorigenic (Table 1). Intraperitoneal CP70sps xenograft tumors were then harvested and subcultured for 7 days to reform spheroids (passage P-1), which were subsequently dissociated and re-injected intraperitoneally into fresh mice. This serial transplantation resulted in tumors from injection of only 100 cells (3/3), and after just one such serial passage, we found tumor latency of 10³ CP70sps cells to decrease from 70 to

41 days, although the same number (10³) of unselected CP70 cells were not tumorigenic, even at nearly twice that time period (Fig. 2A). Also, in accordance with another TIC requisite (reproducible recapitulation of the original tumor histology; refs. 3, 4), all xenograft tumors were similarly categorized as poorly differentiated grades 3 to 4 (Fig. 2B). On the basis of above results, CP70sps meet the currently accepted criteria for stem-like, OTICs and were then used in subsequent drug screening experiments.

Drug screening for inhibitors of CP70sps cells and *in vitro* and *in vivo* testing of selected inhibitors

Growth inhibition of CP70sps was used to screen a library of 1,258 bioactive compounds (LOPAC; Sigma), using the procedure summarized in Fig. 3A. That initial screen identified 61 anti-OTIC compounds (Fig. 3B). Further evaluation of those compounds in growth inhibition assays using lower concentrations resulted in the selection of 2 candidate anti-OTIC agents, of niclosamide and rottlerin, which were then tested using CP70sps and CP70 (Fig. 3C). Although both agents displayed activity, niclosamide was selected for further study, based on our findings of poor *in vivo* activity (data not shown) and previous anticancer studies showing rottlerin to be a poor inhibitor of protein kinase-C isoforms (31). OTIC-selective targeting by niclosamide was further shown by growth inhibition of OTICs derived from CP70 cell line and

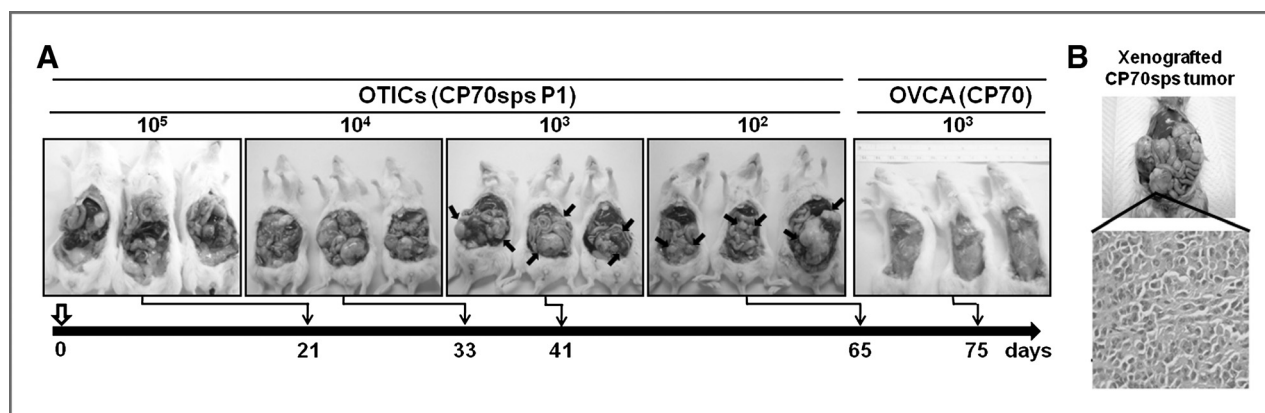


Figure 2. Tumorigenicity and serial transplantation of CP70sps. A, representative results of CP70sps cell serial mouse transplantations. Cell injection numbers are shown above each group of 3 mice. The time durations between engraftment and tumor observation are indicated by black arrows on the timeline shown below. Arrows indicate the tumor nodules. The CP70 injected with 10³ cells, used as a control, is shown in the bottom right panel. B, histopathologic examination of xenograft tumors. Paraffin-embedded sections of tumor nodules were examined by hematoxylin and eosin stain, which confirmed the poorly differentiated ovarian cancer.

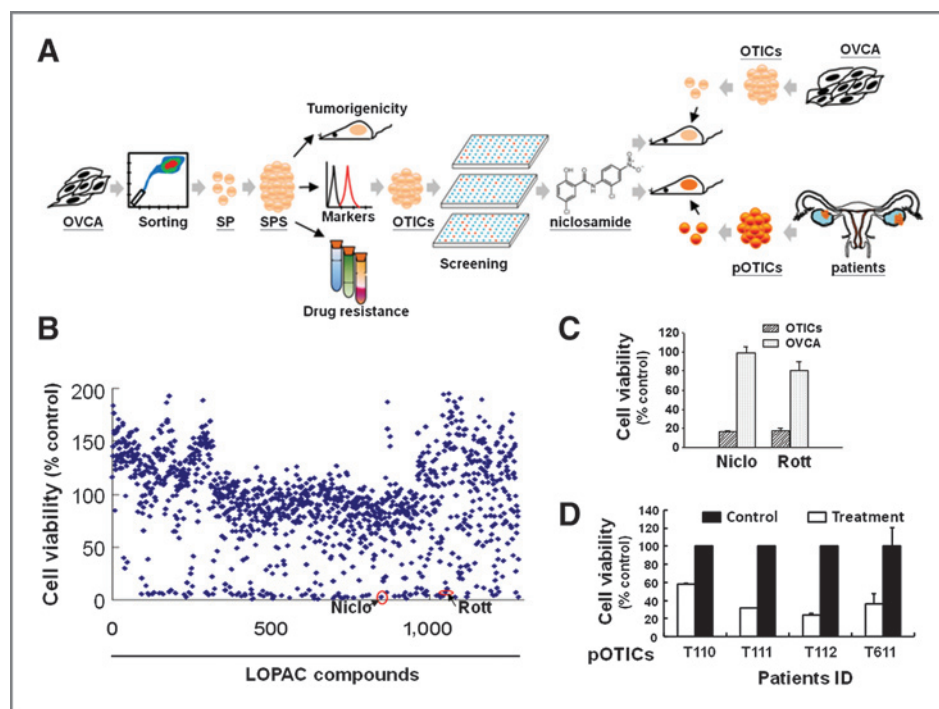


Figure 3. High-throughput screening finds bioactive compounds that possess the capability of OTIC growth inhibition. **A**, a diagram summarizing the logistics of OTIC enrichment and drug screening. A LOPAC library of 1,258 compounds was screened for anti-OTIC activity using an ATP-based cell survival assay at an initial compound concentration of 30 $\mu\text{mol/L}$, resulting in the identification of 61 compounds, which were then further screened at a 10-fold lower dose (3 $\mu\text{mol/L}$). Niclosamide was selected for preclinical experiments *in vitro* and *in vivo* (see text for details). **B**, results of the ATP-based luminescent cell viability assay of the 1,258 compound library, with each blue diamond representing one compound. The X-axis indicates the compound ID, whereas the cell viability is represented by the Y-axis. The 2 compounds with the highest anti-OTIC activity, niclosamide and rottlerin, are circled in red. **C**, growth inhibition of selected compounds in differentiated cancer cells (CP70 cells) and OTICs. Both niclosamide and rottlerin (3 $\mu\text{mol/L}$) preferentially inhibited OTICs over unsorted CP70 cells. Each value represents the mean \pm SD in triplicates. Niclo, niclosamide. Rott, rottlerin. **D**, inhibitory effects of niclosamide on OTICs derived from human ovarian cancer patient tumors [peritoneally derived OTICs (pdOTIC)] in primary culture. pdOTICs were isolated by spheroid formation as previously published by our laboratory, with viability normalized to controls without treatment. Values represent the mean \pm SD in triplicates. All differences shown were statistically significant. $P < 0.05$; Mann-Whitney test.

ovarian cancer patients (peritoneally derived OTICs) *in vitro* (Figs. 3D and 4A).

To assess niclosamide activity against tumor progenitor cells *in vivo*, groups of mice ($n = 3$, each group) were inoculated with 1×10^4 CP70sps cells intraperitoneally and then treated with niclosamide (10 mg/kg/daily), administered intraperitoneally, starting one day after OTIC inoculation. Body weights remained constant during niclosamide treatment (Supplementary Fig. S2), showing a lack of systemic toxicity, whereas body weights of mock-treated mice were significantly increased because of abdominal tumor growth (Fig. 4B). At lower doses (5 mg/kg/daily), niclosamide inhibited OTIC growth within the ovary and partially inhibited growth of OTICs in the peritoneal cavity (Fig. 4C). We also examined whether niclosamide possessed activity against OTIC in the presence of more differentiated tumor cells and observed similar tumor growth inhibition of CP70 cell xenografts in mice treated with niclosamide (Supplementary Fig. S3).

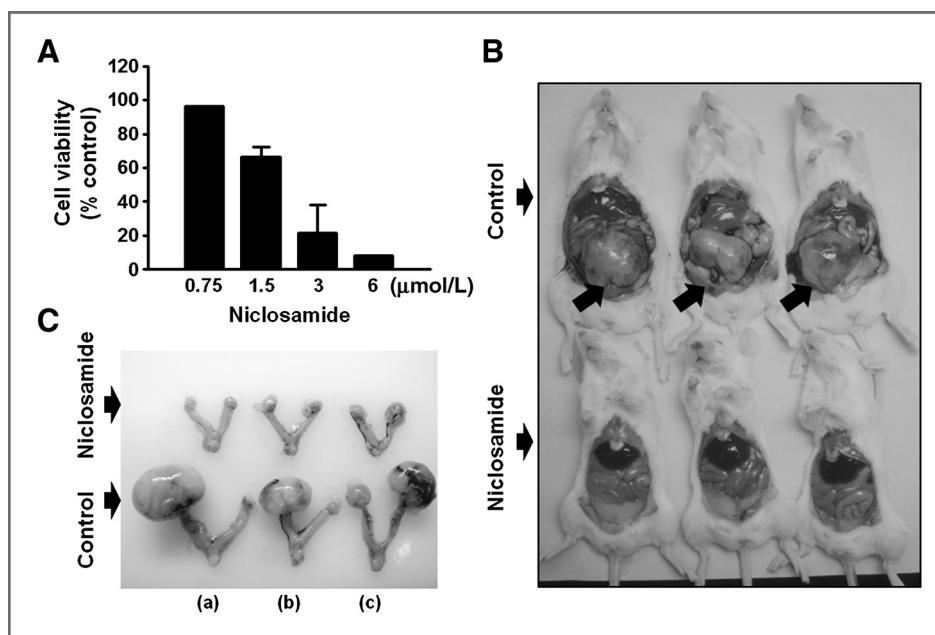
Disruption of OTIC metabolism by niclosamide

Genome-wide gene expression array was subjected to elucidate the mechanism of niclosamide-induced cell

growth inhibition of our cancer stem-like OTICs (R2C1). Significant changes of gene expression in 2,928 genes were identified after niclosamide treatment for different time periods (Fig. 5A). Because uncoupling of mitochondrial oxidative phosphorylation is believed to be its anti-helminthic mechanism of action (32), we hypothesized that niclosamides antagonistic effects on OTICs could, in part, be due to its disruption of metabolism. Consequently, we focused on genes participating in metabolic pathways (oxidative phosphorylation, glycolysis, and fatty acid biosynthesis; Fig. 5B). Our results showed that genes participating in protein complexes of oxidative phosphorylation were downregulated. The shift from oxidative phosphorylation to aerobic glycolysis (i.e., the Warburg effect) is the best characterized metabolic phenotype of cancer (33) and hypothesized to divert carbon into biosynthetic pathways required for high rates of cell proliferation (34). Although gene array results can be informative, functional validation (including enzymatic metabolic assessments) will be necessary for further conclusions with regard to niclosamide metabolic effects.

In particular, the M2 isoform of pyruvate kinase (*PK-M2*), expressed in nearly all cancerous but not normal cells

Figure 4. Niclosamide inhibits the tumor formation of OTICs derived from cancer cell lines *in vivo*. **A**, niclosamide dose-dependent decreases in CP70-derived OTIC viability. OTICs were treated with serially diluted niclosamide (0.75–6 $\mu\text{mol/L}$) and their viability assessed after 2 days. Values represent means \pm SD in triplicates. **B**, OTIC-induced tumor formation is inhibited by niclosamide *in vivo*. Niclosamide treatment (10 mg/kg/daily) was given intraperitoneally every 7 days, starting one day after in NOD/SCID mouse OTIC inoculations and tumor formations following sacrifice after 48 days. Arrowheads indicate the tumors in control group. Mice treated with niclosamide were free from tumor growth. **C**, inhibition of OTIC induced tumor formation on ovary by niclosamide at lower dose (5 mg/kg/daily). Small tumor nodules still grow in the peritoneal cavity.



(34), was found highly upregulated. PK-M2 facilitates the conversion of phosphoenolpyruvate to pyruvate, thus regulating glycolytic intermediates for possible diversion into biosynthetic pathways (34, 35). Interestingly, enzymes important in these biosynthetic pathways were downregulated after niclosamide treatment.

Oxidative stress is another important metabolic regulator and as shown in Fig. 6A, niclosamide treatment resulted in a more than 20% increase in reactive oxygen species (ROS) in cultured OTICs. As elevated ROS is a predominant inducer of mitochondrial apoptosis, we subsequently showed that niclosamide treatment significantly induced apoptosis in human OTICs, as shown by 3 different assays: (i) cytosolic cytochrome C release; (ii) cleavage of AIF1; and (iii) DNA fragmentation determined by PI staining (Fig. 6B and D). Taken together, niclosamide disrupts bioenergetics, biogenesis, and redox regulation in cancer stem-like OTICs.

Discussion

In this study, we carried out a drug screening approach for compounds with activity against cancer stem-like cells designated as OTICs. We discovered that niclosamide, which has proved to be safe and effective for the past 2 decades against numerous parasites, inhibited OTIC growth both *in vitro* and *in vivo*. Our results further suggest that niclosamide represses metabolic enzymes responsible for bioenergetics, biosynthesis, and redox regulation specifically in OTICs, presumably leading to mitochondrial intrinsic apoptosis pathways, loss of tumor stemness, and growth inhibition. In apoptosis cascades, although we found only minor mitochondrial release of cytochrome C, marked release of AIF was observed, suggesting that AIF plays a

major role in niclosamide-associated apoptosis. However, other mechanisms leading to cell death cannot be excluded. Our study further strengthens the concept for therapeutic targeting of cancer stem cells in solid tumors.

Niclosamide is believed to inhibit mitochondrial oxidative phosphorylation (32), and recent research indicates that targeting mitochondria could be an efficient strategy to cancer chemotherapy (36). Niclosamide was reported to inactivate NF- κ B, causing mitochondrial damage and the generation of ROS, leading to apoptosis of leukemic stem cells (37). In another study, both rottlerin and niclosamide were identified in a screen for mTOR-signaling inhibitors (38). In addition, the tuberous sclerosis complex (TSC)–mTOR was reported to maintain stemness properties of HSCs by inhibiting mitochondrial biogenesis and ROS levels (39), implying that mTOR inhibitors (such as niclosamide) may interfere with mitochondria and various metabolic pathways in TICs via disruption of antioxidant responses.

Although mTOR is an important contributor to cancer metabolism (33), in general, the metabolism associated with cancer stemness remains largely unexplored. However, a recent study in lung cancer suggests that TICs possess high mitochondrial membrane potential, low glucose/oxygen consumption, and low ROS and ATP content (40). Thus, interfering with energy production, biosynthesis, and oxidative stress regulation may represent a potential approach for targeting TICs. Compared with our study, biosynthetic diversion of glycolytic intermediates was not examined, and ROS elevation did not evoke apoptosis, but rather autophagy, ERK activation, and caspase-independent cell death (partially mediated by the energy sensor AMPK; ref. 41). Our results, for the first time, show that repression of genes encoding

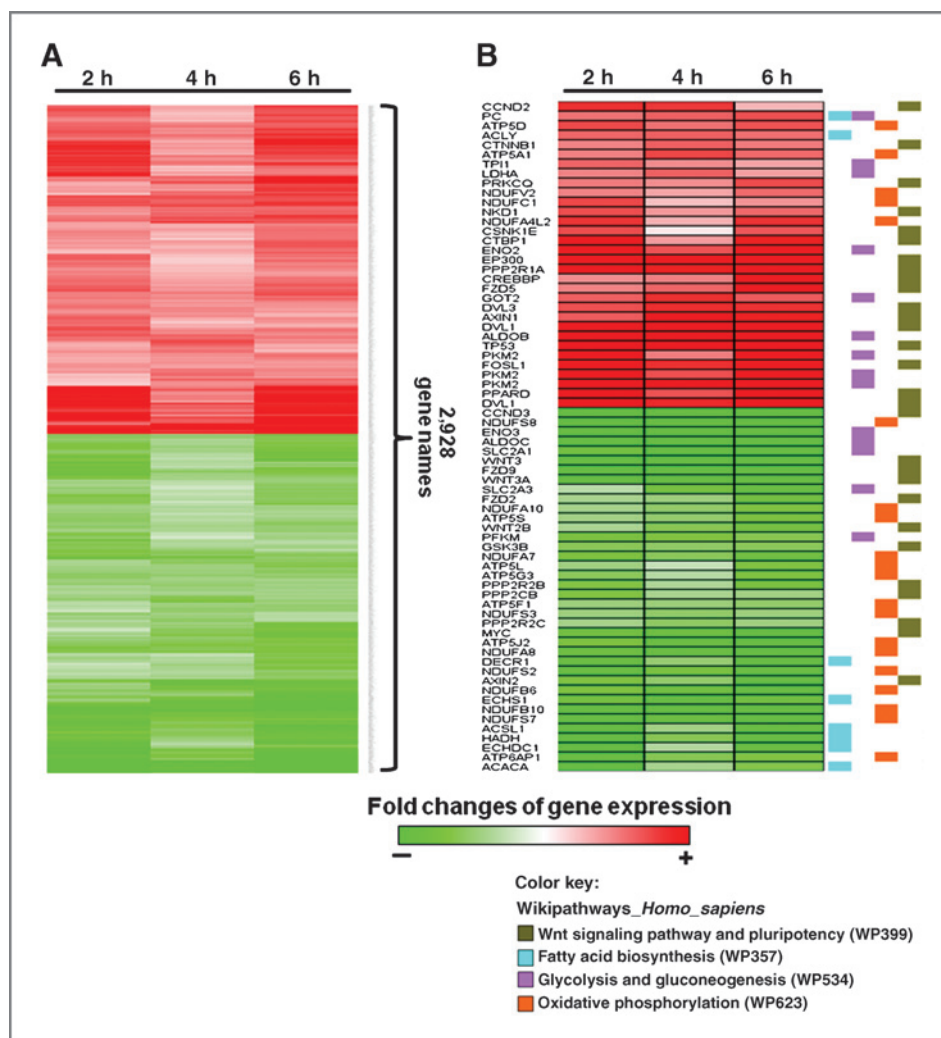


Figure 5. Genome-wide gene expression analysis in niclosamide-treated OTICs. A, the 2,928 genes with significant changes after niclosamide treatment for 2, 4, and 6 hours were shown. The red indicates activation and the green indicates suppression. B, genes participating in metabolism including fatty acid biosynthesis, glycolysis and gluconeogenesis, and oxidative phosphorylation were highlighted.

multiple metabolism enzymes leads to mitochondrial intrinsic apoptosis pathways and inhibition of tumor stemness. As the metabolism of TICs may be different from the bulk population of tumor cells and normal tissues, it may be possible to achieve a therapeutic window for niclosamide, with TIC-specific cytotoxicity and low normal cell toxicity (42, 43).

Embryonic signaling pathways such as Wnt, Hh, and Notch pathways have also been proposed as TIC therapeutic targets (see review ref. 44). We observed Wnt hyperactivity in OTICs, in agreement with previous hypotheses of Wnt inhibitor effectiveness as an ovarian cancer therapy (45). In addition, niclosamide has now been independently identified in screens for Wnt inhibitors (46), via the promotion of Frizzled-1 endocytosis, downregulation of Dishevelled-2, and inhibition of Wnt3A-induced β -catenin stabilization (40, 46), in addition to downregulation of the Wnt/ β -catenin target oncogenes *survivin* and *c-Myc* (47, 48). Likewise, we also observed the downregulation of multiple Wnt ligands/receptors and Wnt target genes *survivin* and *c-Myc* (data

not shown). Several components of another embryogenesis-associated pathway strongly implicated in ovarian carcinogenesis, the cell-to-cell signaling pathway Notch (8), were also suppressed by niclosamide (data not shown). These results agree with another recent niclosamide study in leukemia (49), and it has been widely hypothesized that disruption of Notch signaling may represent a highly effective therapy for ovarian and other solid tumors, via its essentiality to maintaining TIC stemness (50).

In summary, we show that niclosamide has strong inhibitory activity against CP70sps and primary OTICs directly explanted from patient tumors. As a clinically approved drug, further extension of niclosamide to clinical trials may be warranted, allowing clinical assessment of the concept of targeting OTICs, in human ovarian cancer patients. This proof-of-principle study strongly strengthens the rationale for developing highly effective TIC-targeted therapeutics for the management of highly drug-resistant solid tumors, such as epithelial ovarian cancer.

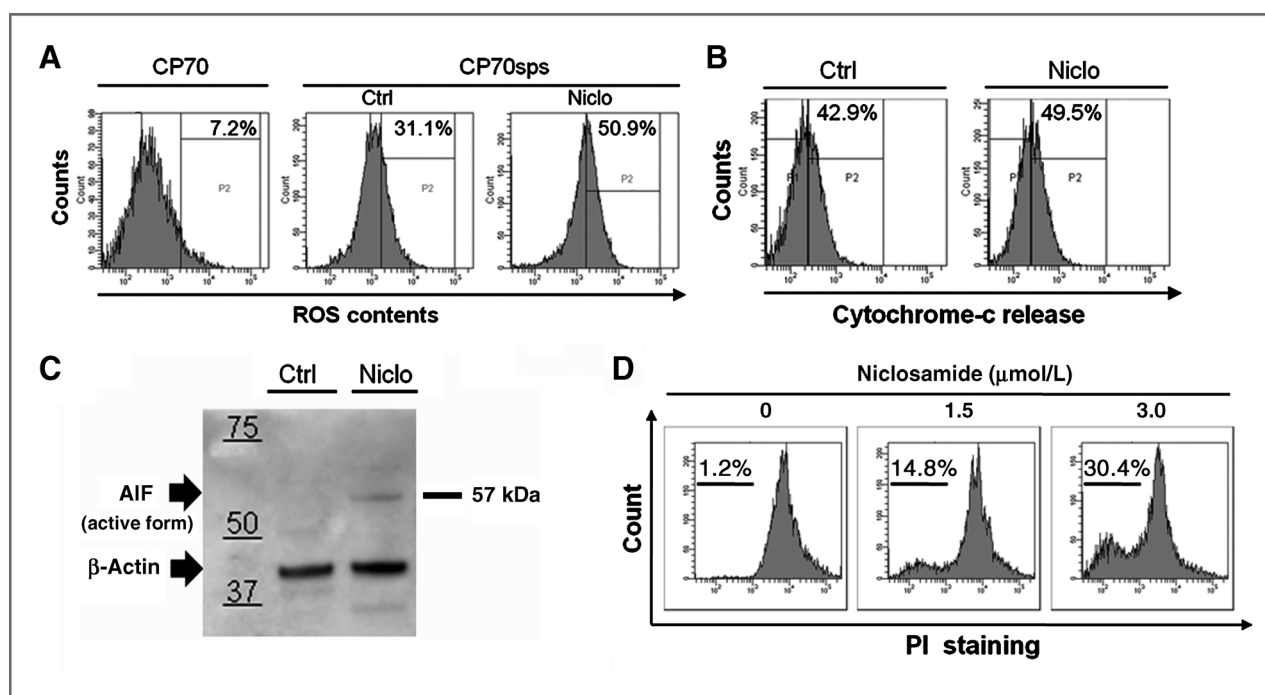


Figure 6. Mechanistic assessments of niclosamide-induced OTICs death. A, oxidative reduction response was assessed by the production of ROS. Mitochondrial-mediated cell death was assessed by 3 different assessments including cytochrome C release (B), cleavage of AIF-1 (C), and DNA fragmentation (D).

Disclosure of Potential Conflicts of Interest

The patent of new indications for cancer therapy using niclosamide is pending. H.-C. Lai is the inventor of the patent.

Authors' Contributions

Conception and design: M.W. Y. Chan, K.P. Nephew, T. Huang, H.-C. Lai
Development of methodology: Y.-T. Yo, Y.-W. Lin, Y.-C. Wang, M.W. Y. Chan, C.-K. Chen, H.-C. Lai

Analysis and interpretation of data (e.g., statistical analysis, biostatistics, computational analysis): Y.-T. Yo, C. Balch, R.-L. Huang, C.-K. Chen, K.P. Nephew, M.-H. Yu, H.-C. Lai

Writing, review, and/or revision of the manuscript: Y.-T. Yo, C. Balch, M.W. Y. Chan, K.P. Nephew, H.-C. Lai

Acquisition of data (provided animals, acquired and managed patients, provided facilities, etc.): Y.-W. Lin, Y.-C. Wang, R.-L. Huang, C.-K. Chen, H.-C. Lai

Administrative, technical, or material support (i.e., reporting or organizing data, constructing databases): Y.-W. Lin, C. Balch, H.-K. Sytwu, C.-C. Chang

Study supervision: M.-H. Yu, H.-C. Lai

Acknowledgments

The authors thank Dr. Ko-Jiunn Liu and Ms. Yi-Mei Hung, National Institute of Cancer Research, National Health Research Institutes, and Ms. Hsin-Yi Lee and Ms. Hui-Chen Wang, Department of Ob/Gyn, Tri-Service General Hospital, Taiwan, Republic of China, for the technical assistance.

Grant Support

This work was supported by grants (NHRI-EX100-9717) from the National Health Research Institute, Taiwan, Republic of China (H.-C. Lai), Teh-Tzer Study Group for Human Medical Research Foundation (H.C. Lai), and U.S. National Cancer Institute awards CA113001 to T. Huang and K.P. Nephew and CA085289 to K.P. Nephew.

The costs of publication of this article were defrayed in part by the payment of page charges. This article must therefore be hereby marked *advertisement* in accordance with 18 U.S.C. Section 1734 solely to indicate this fact.

Received January 4, 2012; revised April 6, 2012; accepted May 3, 2012; published OnlineFirst May 10, 2012.

References

- Jemal A, Siegel R, Xu J, Ward E. Cancer statistics, 2010. *CA Cancer J Clin* 2010;60:277-300.
- Fung-Kee-Fung M, Oliver T, Eliit L, Oza A, Hirte HW, Bryson P. Optimal chemotherapy treatment for women with recurrent ovarian cancer. *Curr Oncol* 2007;14:195-208.
- Dalerba P, Cho RW, Clarke MF. Cancer stem cells: models and concepts. *Annu Rev Med* 2007;58:267-84.
- O'Brien CA, Kreso A, Jamieson CH. Cancer stem cells and self-renewal. *Clin Cancer Res* 2010;16:3113-20.
- Zhang S, Balch C, Chan MW, Lai HC, Matei D, Schilder JM, et al. Identification and characterization of ovarian cancer-initiating cells from primary human tumors. *Cancer Res* 2008;68:4311-20.
- Curley MD, Therrien VA, Cummings CL, Sergent PA, Koulouris CR, Friel AM, et al. CD133 expression defines a tumor initiating cell population in primary human ovarian cancer. *Stem Cells* 2009;27:2875-83.
- Alvero AB, Chen R, Fu HH, Montagna M, Schwartz PE, Rutherford T, et al. Molecular phenotyping of human ovarian cancer stem cells unravels the mechanisms for repair and chemoresistance. *Cell Cycle* 2009;8:158-66.
- Gao MQ, Choi YP, Kang S, Youn JH, Cho NH. CD24+ cells from hierarchically organized ovarian cancer are enriched in cancer stem cells. *Oncogene* 2010;29:2672-80.
- Ren X, Duan L, He Q, Zhang Z, Zhou Y, Wu D, et al. Identification of niclosamide as a new small-molecule inhibitor of the STAT3 signaling pathway. *ACS Med Chem Lett* 2010;1:454-9.
- Dean M, Fojo T, Bates S. Tumour stem cells and drug resistance. *Nat Rev Cancer* 2005;5:275-84.

11. Clarke MF, Dick JE, Dirks PB, Eaves CJ, Jamieson CH, Jones DL, et al. Cancer stem cells—perspectives on current status and future directions: AACR Workshop on cancer stem cells. *Cancer Res* 2006;66:9339–44.
12. Szotek PP, Pieretti-Vanmarcke R, Masiakos PT, Dinulescu DM, Connolly D, Foster R, et al. Ovarian cancer side population defines cells with stem cell-like characteristics and Mullerian Inhibiting Substance responsiveness. *Proc Natl Acad Sci U S A* 2006;103:11154–9.
13. Hu L, McArthur C, Jaffe RB. Ovarian cancer stem-like side-population cells are tumorigenic and chemoresistant. *Br J Cancer* 2010;102:1276–83.
14. Reynolds BA, Weiss S. Clonal and population analyses demonstrate that an EGF-responsive mammalian embryonic CNS precursor is a stem cell. *Dev Biol* 1996;175:1–13.
15. Dontu G, Abdallah WM, Foley JM, Jackson KW, Clarke MF, Kawamura MJ, et al. *In vitro* propagation and transcriptional profiling of human mammary stem/progenitor cells. *Genes Dev* 2003;17:1253–70.
16. Toma JG, McKenzie IA, Bagli D, Miller FD. Isolation and characterization of multipotent skin-derived precursors from human skin. *Stem Cells* 2005;23:727–37.
17. Singh SK, Clarke ID, Terasaki M, Bonn VE, Hawkins C, Squire J, et al. Identification of a cancer stem cell in human brain tumors. *Cancer Res* 2003;63:5821–8.
18. Li C, Heidt DG, Dalerba P, Burant CF, Zhang L, Adsay V, et al. Identification of pancreatic cancer stem cells. *Cancer Res* 2007;67:1030–7.
19. O'Brien CA, Pollett A, Gallinger S, Dick JE. A human colon cancer cell capable of initiating tumour growth in immunodeficient mice. *Nature* 2007;445:106–10.
20. Bast RC Jr, Hennessy B, Mills GB. The biology of ovarian cancer: new opportunities for translation. *Nat Rev Cancer* 2009;9:415–28.
21. Moserle L, Ghisi M, Amadori A, Indraco S. Side population and cancer stem cells: therapeutic implications. *Cancer Lett* 2010;288:1–9.
22. Pastrana E, Silva-Vargas V, Doetsch F. Eyes wide open: a critical review of sphere-formation as an assay for stem cells. *Cell Stem Cell* 2011;8:486–98.
23. Wang YC, Yo YT, Lee HY, Liao YP, Chao TK, Su PH, et al. ALDH1-bright epithelial ovarian cancer cells are associated with CD44, drug resistance, and poor clinical outcome. *Am J Pathol* 2012;180:1159–69.
24. Saeed AI, Sharov V, White J, Li J, Liang W, Bhagabati N, et al. TM4: a free, open-source system for microarray data management and analysis. *Biotechniques* 2003;34:374–8.
25. van Iersel MP, Kelder T, Pico AR, Hanspers K, Coort S, Conklin BR, et al. Presenting and exploring biological pathways with PathVisio. *BMC Bioinformatics* 2008;9:399.
26. Kusumbe AP, Mali AM, Bapat SA. CD133-expressing stem cells associated with ovarian metastases establish an endothelial hierarchy and contribute to tumor vasculature. *Stem Cells* 2009;27:498–508.
27. Silva IA, Bai S, McLean K, Yang K, Griffith K, Thomas D, et al. Aldehyde dehydrogenase in combination with CD133 defines angiogenic ovarian cancer stem cells that portend poor patient survival. *Cancer Res* 2011;71:3991–4001.
28. Strauss R, Li ZY, Liu Y, Beyer I, Persson J, Sova P, et al. Analysis of epithelial and mesenchymal markers in ovarian cancer reveals phenotypic heterogeneity and plasticity. *PLoS One* 2011;6:e16186.
29. Kusumbe AP, Bapat SA. Cancer stem cells and aneuploid populations within developing tumors are the major determinants of tumor dormancy. *Cancer Res* 2009;69:9245–53.
30. Quintana E, Shackleton M, Sabel MS, Fullen DR, Johnson TM, Morrison SJ. Efficient tumour formation by single human melanoma cells. *Nature* 2008;456:593–8.
31. Soltoff SP. Rottlerin: an inappropriate and ineffective inhibitor of PKCdelta. *Trends Pharmacol Sci* 2007;28:453–8.
32. Pearson RD, Hewlett EL. Niclosamide therapy for tapeworm infections. *Ann Intern Med* 1985;102:550–1.
33. Cairns RA, Harris IS, Mak TW. Regulation of cancer cell metabolism. *Nat Rev Cancer* 2011;11:85–95.
34. Vander Heiden MG, Cantley LC, Thompson CB. Understanding the Warburg effect: the metabolic requirements of cell proliferation. *Science* 2009;324:1029–33.
35. Christofk HR, Vander Heiden MG, Wu N, Asara JM, Cantley LC. Pyruvate kinase M2 is a phosphotyrosine-binding protein. *Nature* 2008;452:181–6.
36. Galluzzi L, Larochette N, Zamzami N, Kroemer G. Mitochondria as therapeutic targets for cancer chemotherapy. *Oncogene* 2006;25:4812–30.
37. Jin Y, Lu Z, Ding K, Li J, Du X, Chen C, et al. Antineoplastic mechanisms of niclosamide in acute myelogenous leukemia stem cells: inactivation of the NF-kappaB pathway and generation of reactive oxygen species. *Cancer Res* 2010;70:2516–27.
38. Balgi AD, Fonseca BD, Donohue E, Tsang TC, Lajoie P, Proud CG, et al. Screen for chemical modulators of autophagy reveals novel therapeutic inhibitors of mTORC1 signaling. *PLoS One* 2009;4:e7124.
39. Chen C, Liu Y, Liu R, Ikenoue T, Guan KL, Liu Y, et al. TSC-mTOR maintains quiescence and function of hematopoietic stem cells by repressing mitochondrial biogenesis and reactive oxygen species. *J Exp Med* 2008;205:2397–408.
40. Ye XQ, Li Q, Wang GH, Sun FF, Huang GJ, Bian XW, et al. Mitochondrial and energy metabolism-related properties as novel indicators of lung cancer stem cells. *Int J Cancer* 2011;129:820–31.
41. Alvero AB, Montagna MK, Holmberg JC, Craveiro V, Brown D, Mor G. Targeting the mitochondria activates two independent cell death pathways in ovarian cancer stem cells. *Mol Cancer Ther* 2011;10:1385–93.
42. Merschjohann K, Steverding D. *In vitro* trypanocidal activity of the anti-helminthic drug niclosamide. *Exp Parasitol* 2008;118:637–40.
43. Osada T, Chen M, Yang XY, Spasojevic I, Vandeusen JB, Hsu D, et al. Antihelminth compound niclosamide downregulates Wnt signaling and elicits antitumor responses in tumors with activating APC mutations. *Cancer Res* 2011;71:4172–82.
44. Takebe N, Ivy SP. Controversies in cancer stem cells: targeting embryonic signaling pathways. *Clin Cancer Res* 2010;16:3106–12.
45. Paul S, Dey A. Wnt signaling and cancer development: therapeutic implication. *Neoplasia* 2008;55:165–76.
46. Chen M, Wang J, Lu J, Bond MC, Ren XR, Lyerly HK, et al. The anti-helminthic niclosamide inhibits Wnt/Frizzled1 signaling. *Biochemistry* 2009;48:10267–74.
47. Ma H, Nguyen C, Lee KS, Kahn M. Differential roles for the coactivators CBP and p300 on TCF/beta-catenin-mediated survivin gene expression. *Oncogene* 2005;24:3619–31.
48. Calvisi DF, Conner EA, Ladu S, Lemmer ER, Factor VM, Thorgeirsson SS. Activation of the canonical Wnt/beta-catenin pathway confers growth advantages in c-Myc/E2F1 transgenic mouse model of liver cancer. *J Hepatol* 2005;42:842–9.
49. Wang AM, Ku HH, Liang YC, Chen YC, Hwu YM, Yeh TS. The autonomous notch signal pathway is activated by baicalin and baicalin but is suppressed by niclosamide in K562 cells. *J Cell Biochem* 2009;106:682–92.
50. Androutsellis-Theotokis A, Leker RR, Soldner F, Hoepfner DJ, Ravin R, Poser SW, et al. Notch signalling regulates stem cell numbers *in vitro* and *in vivo*. *Nature* 2006;442:823–6.

Molecular Cancer Therapeutics

Growth Inhibition of Ovarian Tumor–Initiating Cells by Niclosamide

Yi-Te Yo, Ya-Wen Lin, Yu-Chi Wang, et al.

Mol Cancer Ther 2012;11:1703-1712. Published OnlineFirst May 10, 2012.

Updated version Access the most recent version of this article at:
doi:[10.1158/1535-7163.MCT-12-0002](https://doi.org/10.1158/1535-7163.MCT-12-0002)

Supplementary Material Access the most recent supplemental material at:
<http://mct.aacrjournals.org/content/suppl/2012/05/10/1535-7163.MCT-12-0002.DC1.html>

Cited articles This article cites 50 articles, 15 of which you can access for free at:
<http://mct.aacrjournals.org/content/11/8/1703.full.html#ref-list-1>

Citing articles This article has been cited by 2 HighWire-hosted articles. Access the articles at:
<http://mct.aacrjournals.org/content/11/8/1703.full.html#related-urls>

E-mail alerts [Sign up to receive free email-alerts](#) related to this article or journal.

Reprints and Subscriptions To order reprints of this article or to subscribe to the journal, contact the AACR Publications Department at pubs@aacr.org.

Permissions To request permission to re-use all or part of this article, contact the AACR Publications Department at permissions@aacr.org.